

Electronic Supplementary Information 1

Poisson-Boltzmann model for the partition of highly charged macromolecular co-ion probes

Context

The aim of this supplementary information section is to provide the details for modelling the partition coefficients of highly charged, macromolecular co-ion probes in highly charged hydrogels.

The basic approach to model the partition of highly charged macromolecular probes into like-charged hydrogels is given in the main text: the potential distribution inside the pores is obtained by numerical solution of equation 1, with boundary conditions given by eq. 2 and a local charge density given by eq. 5 and eq. 6-B. The partition coefficient is then obtained by integration of the local partition coefficients over the channel width, as indicated by eq. 8, with the appropriate number of charges per probe molecule n .

In practice, there is however a number of additional difficulties associated with the partition of macromolecular probes, which we address in turn in this electronic supplementary information section.

Molecular Weight Distribution

While some macromolecules such as proteins show a highly defined, monodisperse molecular weight, others, namely many natural or man-made polymers, show a high degree of polydispersity. Given the exponential dependence of the partition coefficients on the number of charges at a given electric potential, the simultaneous presence of molecules with very different molecular weights and therefore charge number n should be taken into account. In our case, we used Gel Permeation Chromatography (GPC 50+ Agilent, eluent NaNO_3 10mM + 10% MeOH, PL aquagel-OH, MIXED-M, Universal calibration), to determine the molecular weight distribution for the fluorescently labelled alginate probe. Fig. S1 shows the results.

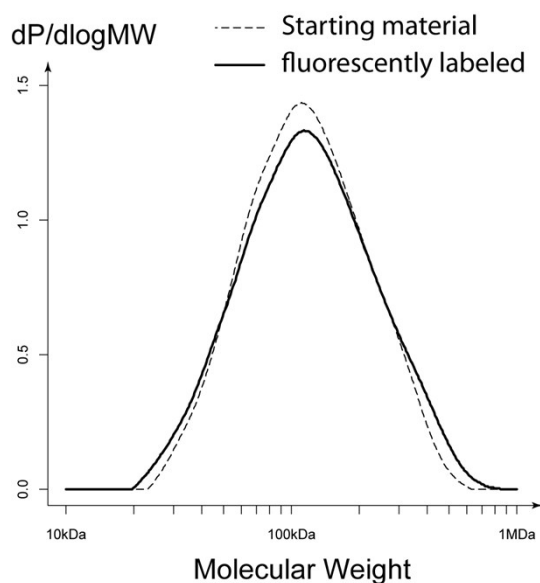


Figure S1: Molecular weight distribution of the fluorescently labelled alginate probe. The number average was $M_n=94.8\text{kDa}$, the weight average was $M_w=147.8\text{kDa}$, corresponding to a polydispersity index of 1.56. The molecular weight distribution was similar to the one measured prior to fluorescent labelling (dashed line, $M_n=110.1\text{kDa}$, $M_w=137.9\text{kDa}$, $PD=1.44$), the main influence of the labelling being a slight peak broadening. No molecular weight fragments with a mass below 19.6kDa are detected, indicating very efficient removal of free label.

Alginate is a mixed co-polymer of guluronic and mannuronic acid¹, and since guluronic acid and mannuronic acid are stereoisomers with identical molecular weight, the molecular weight per residue is 198g/mol when provided as sodium salt. Hence, for each molecular weight present in the probe, the number of elementary charges n can be calculated by:

$$n = -M/(198\text{g/mol}) \quad (\text{S2})$$

where M is the molecular weight of the alginate fraction under consideration. It is then a matter of integration of the partition coefficients K as evaluated by eq. 8 over the different molecular weight classes present in the sample, taking into account the fraction of the total mass present in each class. For the ionic exclusion of co-ions examined here, taking into account the molecular weight distribution leads to substantially higher predicted partition coefficients than when using only the average molecular weight, particularly under conditions of highly efficient exclusion (small pore size, low ionic force). This is because the smaller, and therefore less charged fragments, are much less efficiently excluded; the highly nonlinear nature of the Boltzmann exponentials then leads to a dramatic increase in the overall partition coefficient.

Counterion Condensation

According to the Manning counterion condensation theory, a tightly bound cloud of counter-ions is formed around polyelectrolytes with a linear charge density exceeding one elementary charge per Bjerrum length^{2,3}. The Bjerrum length is 0.7nm in water at ambient temperature³, whereas the hexose moieties making

up the alginate chains have a molecular size on the order of 0.4nm⁴, such that indeed one may suspect a significant shielding effect due to the presence of a localized counter-ion cloud.

In terms of the electrostatic interaction between the probe and the charged gel, the presence of counterion condensation can be dealt with by calculating the electrostatic repulsion energy effectively experienced by the probe, and comparing it to the energy obtained by the local potential and the charge of probe⁵. To obtain the electrostatic repulsion energy experienced by the probe, one needs to calculate the electrostatic energy of the combined gel/probe system, and then subtract the sum of the electrostatic energies associated when the two are taken alone (eq. 52 in ⁵):

$$\Delta G = G_{\text{probe and gel}} - G_{\text{probe}} - G_{\text{gel}} \quad (\text{S3})$$

The relevant apparent charge density can then be calculated by comparing the electrostatic repulsion energy calculated by eq. S3 to the theoretical repulsion energy, were there no counterion condensation effect:

$$n_{\text{apparent}} = n^* \Delta G / (\Phi^* Q) \quad (\text{S4})$$

where Φ is the potential at the position of the probe, but calculated in the absence of the probe (gel only), and Q the charge of the simulated probe element. The calculation of the free energy of a charged element in the presence of an ionic buffer obeying the Poisson-Boltzmann law is well known, it amounts to calculating the progressively larger electrostatic energy necessary to bring the fixed space charge into its position during a virtual charging process (eq. 22 in ⁶):

$$G = \int_0^{Q_{\text{final}}} \int \Phi(Q, x) dx dQ \quad (\text{S5})$$

where we have added the spatial integration to account for volumetric charge density rather than surface charge as in ⁶, and where Q_{final} is the total charge necessary to obtain the final desired space charge distribution, while Q is the current charge already applied, and x the spatial coordinate of the 1D model we use. The essence of eq. 5 is that we should start out with the simulation region without charges, and therefore $\Phi=0$ everywhere. Then, a small fraction of the final space charge density is added, corresponding to some total amount of charge Q , and the electrical potential Φ is evaluated for the resulting space distribution by applying the Poisson-Boltzmann equation (eq. 1 in the main text) and suitable boundary conditions for periodicity and therefore charge neutrality (eq. 2). The newly calculated potential distribution $\Phi(Q, x)$ is then used for the evaluation of the free energy change associated with the next addition of space charge density, and by progressively raising the fixed charge density to its final value, while summing up the rising contributions of each new bit of charge added, one gets the free electrostatic energy of the desired fixed charge distribution. The procedure is generic and does not depend on the particular fixed charge density distribution, such that it can be used to calculate the

different free energy values in eq. S3 by simple variation of the desired final fixed charge distribution.

In terms of the predicted partition coefficients, taking the electrostatic shielding arising through counterion condensation lowers the calculated repulsion energy, and thus decreases co-ion exclusion efficiency further.

Given the rather involved numerical calculations necessary to assess the effect of counterion condensation, we calculate the apparent charge number n_{apparent} for each experimental or theoretical condition for the probe molecule being located at the channel midline. We then use n_{apparent} , which is typically in the range of 0.1 to 0.3 times the true charge number n under our experimental conditions, for all molecular weights and potential positions of the probe. The approach is motivated by the fact that for highly charged co-ion probes, by far the highest concentration is expected near the channel midline, with only minor contributions towards the channel walls.

Pore size distribution

The Ogston model predicts that the pore radius should follow a X distribution with 2 degrees of liberty, also referred to as square root of a X^2 -distribution⁷:

$$\frac{dP}{dr} = 2\Gamma\left(\frac{3}{2}\right)^2 \cdot \frac{r}{r_0^2} \cdot \exp\left[-\left(\frac{r}{r_0}\right)^2 \cdot \Gamma\left(\frac{3}{2}\right)^2\right] \quad (\text{S6})$$

where P is the cumulative probability of the pore size distribution, Γ is the gamma function, and where the scaling is chosen such that the arithmetic mean of the radius is given by r_0 .

As for the molecular weight distribution, taking into account the pore size distribution is done numerically by evaluation of the partition coefficient for each pore size, and then integration by using the probabilities of the different pore sizes.

Due to the non-linearity of the Boltzmann exponentials, we find that using the Ogston pore distribution leads to increased predicted values for the partition coefficients of the co-ion probes, in particular in circumstances with strong ionic exclusion effects, since the larger pores offer a refuge for otherwise efficiently excluded probe molecules.

Bibliography

1. D. A. Rees and J. W. B. Samuel, *J Chem Soc C*, 1967, 2295-&.
2. G. S. Manning, *Chem. Phys.*, 1969, **51**, 924.
3. W. B. Russel, D. A. Saville and W. R. Schowalter, *Colloidal Dispersions*, Cambridge University Press, New York, 1989.
4. S. G. Schulz and A. K. Solomon, *J Gen Physiol*, 1961, **44**, 1189-1199.
5. E. M. Johnson, in *Massachusetts Institute of Technology*, Cambridge, 1995.
6. E. J. W. Verwey and J. T. G. Overbeek, *Theory of the stability of lyophobic colloids*, Elsevier, Amsterdam, 1948.
7. D. Rodbard and A. Chrambach, *Proc Natl Acad Sci U S A*, 1970, **65**, 970-977.